Spatial Modulation in the Underwater Acoustic Channel

Daniel Kilfoyle
SAIC
phone: 508-274-1197
email: daniel.b.kilfoyle@saic.com

Abstract Multiple-input multiple-output (MIMO) communication channels are an active area of research for terrestrial wireless applications. The natural bandwidth limitations of the underwater acoustic channel (UAC) combined with the potential for a rich spatial propagation structure suggest the ocean may be another useful application area for MIMO techniques.

An underwater acoustic communications experiment was conducted in the waters surrounding Elba, Italy, using spatially modulated signals. Two frequency regimes (9.5–14.5 kHz and 25–35 kHz) were explored over ranges up to 5 km using vertical line arrays suspended from drifting ships. The UAC had an average depth of 100 m. One-way communication links were established at two sites with one site having a rocky (reverberant) bottom and the other having a muddy (absorbent) bottom.

The waveform comprised a single data stream with concatenated codes providing error control. The inner code was a high rate BCH code. Trellis-coded modulation was used as the basis for the outer code. Successive coded symbols were multiplexed across the available transducer elements. This coding approach effectively maintains the inherent bandwidth efficiency of MIMO signaling.

The receiver was an adaptive recursively updated multichannel decision feedback equalizer operating in conjunction with a digital phase-locked loop. A packet-based, transport architecture was used and included a training sequence. A Viterbi algorithm was integrated with the equalizer that supported simultaneous tap-weight update and trellis transversal, thereby affording the decision-directed update partial error control.

Using appropriate assumptions, channel capacity using a single transducer was estimated to be 5.4 bits/channel use at the soft bottom site. Capacity was maximized at 15.9 bits/channel use using four transducers. More detailed results will be presented along with performance predictions based on both propagation models and measured channel transfer functions.

Report Documentation Page

Form Approved
OMB No. 0704-0188

1. REPORT DATE	2. REPORT TYPE	3. DATES COVERED
20 DEC 2004	**N/A**	**-**

4. TITLE AND SUBTITLE	5a. CONTRACT NUMBER
Spatial Modulation in the Underwater Acoustic Channel	5b. GRANT NUMBER
	5c. PROGRAM ELEMENT NUMBER
6. AUTHOR(S)	5d. PROJECT NUMBER
	5e. TASK NUMBER
	5f. WORK UNIT NUMBER
7. PERFORMING ORGANIZATION NAME(S) AND ADDRESS(ES) **SAIC**	8. PERFORMING ORGANIZATION REPORT NUMBER
9. SPONSORING/MONITORING AGENCY NAME(S) AND ADDRESS(ES)	10. SPONSOR/MONITOR'S ACRONYM(S)
	11. SPONSOR/MONITOR'S REPORT NUMBER(S)

12. DISTRIBUTION/AVAILABILITY STATEMENT
Approved for public release, distribution unlimited

13. SUPPLEMENTARY NOTES
See also, ADM001741 Proceedings of the Twelfth Annual Adaptive Sensor Array Processing Workshop, 16-18 March 2004 (ASAP-12, Volume 1)., The original document contains color images.

14. ABSTRACT

15. SUBJECT TERMS

16. SECURITY CLASSIFICATION OF:			17. LIMITATION OF ABSTRACT	18. NUMBER OF PAGES	19a. NAME OF RESPONSIBLE PERSON
a. REPORT **unclassified**	b. ABSTRACT **unclassified**	c. THIS PAGE **unclassified**	**UU**	**20**	

SPATIAL MODULATION IN THE UNDERWATER ACOUSTIC CHANNEL

Daniel Kilfoyle, Science Applications International Corporation
406 Sippewissett Road, Falmouth, MA 02540 Daniel.B.Kilfoyle@saic.com
Lee Freitag, Woods Hole Oceanographic Institution

ABSTRACT

Multiple-input / multiple-output (MIMO) communication channels are an active area of research for terrestrial wireless applications. The natural bandwidth limitations of the underwater acoustic channel (UAC) combined with the potential for a rich spatial propagation structure suggests the ocean is another useful application area for MIMO techniques. An underwater acoustic communications experiment was conducted in the waters surrounding Elba, Italy, using spatially modulated signals. Two frequency regimes (9.5 – 14.5 kHz and 25 – 35 kHz) were explored over ranges up to 5 km using vertical line arrays. One-way communication links were established at two sites with one site having a rocky (reverberant) bottom and the other having a muddy (absorbent) bottom. The waveform comprised a single data stream with concatenated codes providing error control. The receiver was an adaptive recursively updated multi-channel decision feedback equalizer operating in conjunction with a digital phase locked loop. Channel capacity using a single transducer was estimated to be 7.6 bits/channel use at the soft bottom site. Capacity was maximized at 23.0 bits/channel use using four transducers at that site. While the receiver was effective, the ability of the equalizer to cope with channel dispersion effects was a limiting factor.

I. INTRODUCTION

Underwater acoustic communication provides a unique capability that is important to many users in both government and private industry. At the same time, the dynamic and dispersive nature of the underwater acoustic channel (UAC) has limited demonstrated data rates to well below those common to other systems such as landline and wireless [1], particularly for horizontal propagation paths. With fundamental limits on bandwidth, mostly dictated by the attenuation characteristics of sea water [2], increasing spectral efficiency, defined as the ratio of data rate to signal bandwidth, is an important approach to increasing data rates. The successful demonstration of phase coherent signaling [3] was a milestone in the field as it enabled bandwidth efficiencies of two or more over practical long-range horizontal communication paths. The exploitation of the ocean's rich spatial structure through the use of spatial modulation can provide significant additional bandwidth efficiency gains.

The UAC exhibits stressing traits that have yet to surface, for the most part, in terrestrial wireless MIMO channels. Temporal dispersion due to the waveguide nature of the UAC leads to impulse responses that often extend from $10/B$ to $100/B$ in duration, where B is the signal bandwidth. In contrast, urban spread spectrum systems such as those conforming to the IS-95B and 1XRTT standards rarely see significant multipath extents beyond $10/B$. Frequency dispersion due to sea surface motion, platform movement, and even seawater currents and turbulence often lead to coherence times of $100/B$. In contrast, a vehicle traveling 30 m/s while operating a PCS-band phone can expect coherence times of nearly $10000/B$. These conditions demand sophisticated equalizer structures with rapid adaptation rates. Algorithms developed by the underwater acoustic telemetry community may prove valuable when terrestrial wireless MIMO systems inevitably migrate to ultra-high bandwidth, mobile applications.

In this paper, the relatively mature equalizer structure developed for the UAC is extended to support MIMO signaling and validated in sea trials. In section I, the baseline algorithm is described. The motivation for a particular error coding strategy is presented. In section III, details of the at-sea testing procedure used near Elba, Italy, during October 2003, are given. Section IV reviews the estimated channel capacity increases provided by the use of spatial modulation, showing its effectiveness, while pointing out the limitations imposed by channel dispersion. The final section will summarize the key ideas addressed in this paper.

II. EQUALIZER DESIGN

For the purpose of receiver design, communication via spatial modulation is a form of multi-user communication where there is the possibility of introducing dependency between different users. Rather than relying on frequency division multiple access (FDMA) or code division multiple access (CDMA) techniques, the spatial modulation receiver separates signals by using the differing spatial signatures of the data streams to separate them. The demodulation algorithm used in these experiments is based on the multi-user receiver structure described by Stojanovic and Zvonar [4]. A number of similar and competing equalizer structures are described in the literature [5].

Referring to figure 1, the first step is a coarse timing and carrier synchronization typically done via correlating with a training sequence appended to each packet of symbols. The equalization and channel separation task is accomplished with the joint application of tapped delay lines on each received signal, decision feedback filters for all data streams, and a digital phase locked loop. Decisions are based on a minimum Euclidian distance metric that compares the symbol estimate vector to a map of valid messages. The decisions are made with a Viterbi algorithm that operates in concert with the equalizer on a symbol-to-symbol basis. Soft decisions with low latency (typically less than 10 symbols) are released to support the filter update while hard decisions are released with a higher latency. The general area of delayed decision feedback sequence estimation is addressed by Duel-Hallen [6].

The essential difference between this receiver and a typical multi-user decision feedback equalizer is the integration of the Viterbi algorithm with the adaptation process and the inclusion of feedback filtering within the Viterbi trellis. Note that the diagram shown in figure 4 is only intended to show the processing for one data stream. More specifically, ν_j is the received data for the j^{th} receiver element. T_s is the symbol interval. N_1 and N_2 are the durations, before and after the timing reference, that have delay tap support. a_{ki} is the linear

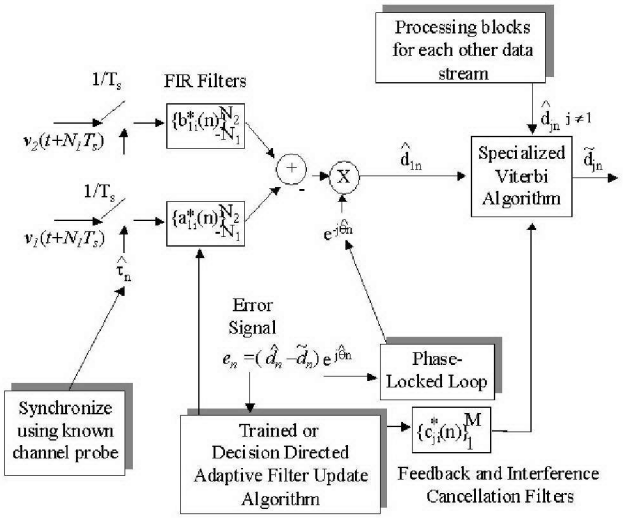

Figure 1. The receiver algorithm is schematically depicted here. The variables and functions are described in the text.

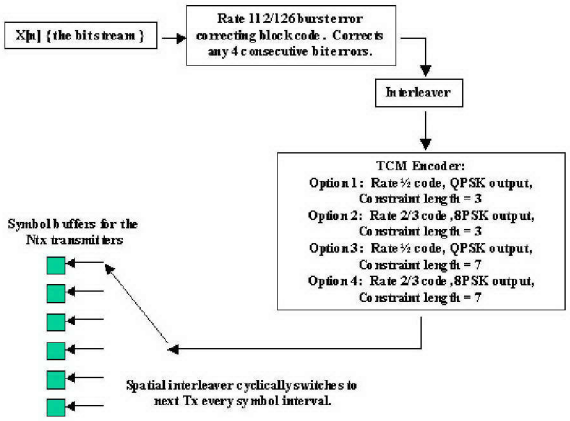

Figure 2. The concatenated coding process that maps information bits to symbols for each transducer is shown here. The key components are an outer block code, an interleaver, and an inner trellis-coded modulation encoder.

transversal filter for the k^{th} data stream and the i^{th} symbol interval for the first receive element. b_{ki} is the linear transversal filter for the k^{th} data stream and the i^{th} symbol interval for the second receive element. The architecture is readily generalized to include more receiver elements. c_{ki} is the linear transversal feedback filter for the k^{th} data stream and the i^{th} symbol interval for the second receive element. Each data stream has a unique feedback filter containing previous decisions for all other data streams and a unique phase correction. Similar processing blocks for the other data streams then feed their estimates to a specialized Viterbi algorithm that traverses one stage in its trellis before releasing a soft decision and a hard decision for one symbol of each of the data streams.

An important element of the receiver is the extension of the decision feedback filter to include taps for the current symbols of all the data streams. In the decision process, those taps are repeatedly filled with the symbols of the message being considered as a candidate for decision. This is similar to the processing required for the maximum likelihood receiver. The feature is particularly important if the channel gains imparted to each data stream vary significantly such as with near-far behavior. Interference cancellation in this manner is similar to that implemented in the so-called D-BLAST architecture except that the cancellation is done jointly rather than sequentially [7].

A wide variety of possibilities exist for space-time coding strategies. For these experiments, a single bit stream was coded via concatenated coding. A high rate outer block code was first used followed by an interleaver to provide protection against burst errors. The resultant, encoded bit stream was then convolutionally encoded with a trellis-coded modulation algorithm [8]. Successive coded symbols were then mapped to successive transducers as in figure 2. The use of concatenated codes which combine a space-time code with an outer encoder has been shown to offer robust performance in MIMO channels with correlated fading [9]. The signal design used has several advantages that make it well suited to underwater acoustic communication applications. First, the overall coding efficiency is high (89%) which maintains the advantage of high spectral efficiency that spatial modulation offers. Second, the inner convolutional code structure supports joint equalization and Viterbi decoding thereby giving the adaptive filter update process the benefit of coding gain. Finally, by introducing dependency between the transmitted data streams, tolerance to shadowing or fading of the signal from any one transducer is created. As many important UAC telemetry applications are inter-symbol interference limited rather than power limited, the coupling of coding gain to the equalizer update process is crucial. Furthermore, the catastrophic failure mode of recursive adaptive equalizers in the UAC makes them ill-suited to iterative decoding approaches which alternately perform equalization and decoding.

III. ELBA 2003 TEST DESCRIPTION

The NATO Undersea Research Centre, SAIC, SPAWAR, the University of Delaware, and the Woods Hole Oceanographic Institution conducted a collaborative sea trial in the waters off of Elba, Italy, between October 27 and October 30, 2003. This cruise sought to improve understanding of the propagation and scattering of high frequency acoustic waves (5-50 kHz) in the presence of oceanographic variability in shallow water regions [10]. In this paper, only the test aspects directly related to testing of spatial modulation in the UAC will be discussed.

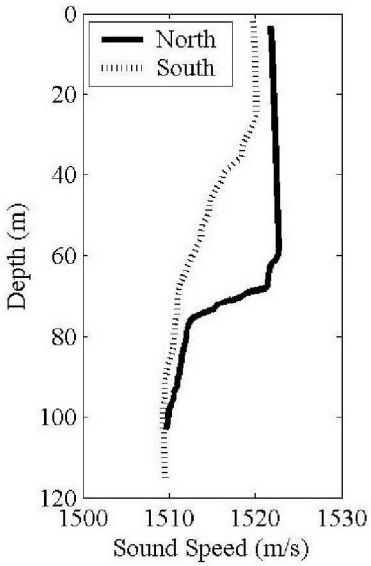

Figure 3. The sound speed profiles at both sites were downward refracting with a weak surface duct. The north site bottom layer transition was quite abrupt.

Table 1. Post-equalization SNR for various levels of spatial modulation is shown here for the low frequency band at a range of 2.1 km at the North site. C has units of bits/channel use.

	1 Chan	2 Chan	3 Chan	4 Chan	5 Chan	6 Chan
SNR_{out} (dB)	16.1	11.4	8.7	7.4	5.3	3.7
	-	9.8	5.0	3.3	1.8	0.4
	-	-	7.7	5.9	2.3	1.6
	-	-	-	5.8	3.6	1.8
	-	-	-	-	4.3	3.0
	-	-	-	-	-	1.3
C	4.8	6.5	7.3	10.6	9.7	9.4

Table 2. Post-equalization SNR for various levels of spatial modulation is shown here for the low frequency band at a range of 2.5 km at the South site. C has units of bits/channel use.

	1 Chan	2 Chan	3 Chan	4 Chan	5 Chan	6 Chan
SNR_{out} (dB)	23.5	19.1	16.3	13.0	9.1	6.0
	-	20.6	18.0	14.7	12.3	9.9
	-	-	17.2	13.8	11.3	5.0
	-	-	-	13.8	12.3	9.4
	-	-	-	-	8.4	3.9
	-	-	-	-	-	8.3
C	7.6	13.1	17.1	23.0	21.9	17.6

The test assets included the R/V Alliance, which hosted a 14-element flexible hydrophone vertical line array (VLA) with 1 m spacing and a 12 element rigid hydrophone VLA with a 15 cm spacing. Each hydrophone array was sufficiently wideband to record all signals transmitted. Two transducer arrays were hosted by the vessel Saralu including a 6 element, 2 m spaced, array tuned for operation between 9.5 and 14 kHz and a 3 element, 53 cm spaced, transducer array tuned for operation between 25 and 35 kHz. Packet-based waveforms were alternately transmitted in both frequency bands. An average power constraint was imposed. Testing parameters included the number of simultaneous, unique spatially multiplexed packets (1 to 6 at the mid-band and 1 to 3 at the high band) and symbol constellation size (4, 8, and 16-level quadrature amplitude modulation).

The two test sites were utilized specifically to provide contrasting environments that would aid understanding how propagation physics and communication performance are related. The site to the North of Elba had a nominal water column depth of 100 m with hard, reverberant bottom structure. The site to the South of Elba also had a nominal depth of 100 m but had substantial sediment deposits leading to severe bottom attenuation. Typical sound velocity profiles from each site are seen in figure 3. Each site exhibited a warm surface layer atop a cooler bottom layer with an exceptionally steep gradient at the north site between the layers.

IV. RESULTS

In general, spatial modulation was more effective at the South site than at the North site. The effectiveness of the proposed receiver for each site will first be described. The observed differences will then be discussed in terms of the propagation conditions, namely time and frequency dispersion.

A useful metric to characterize potential communication performance is the post-equalization signal-to-noise ratio (SNR_{out}) of the data prior to the decision device. By processing the packet continually in training mode, system performance can be extrapolated from SNR_{out} to arbitrary coding strategies. With appropriate assumptions, one may even estimate the capacity given SNR_{out}. Assuming that the equalizer both whitens the residual noise and any channel-

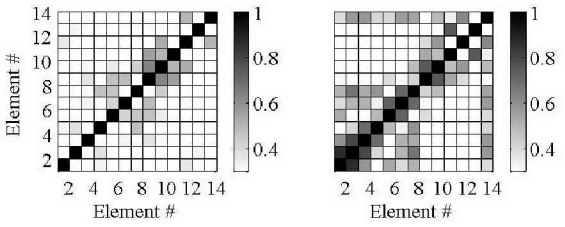

Figure 4. The array spatial covariance matrix for the low-band transmissions at the North site (left panel) and the South site (right panel) are shown.

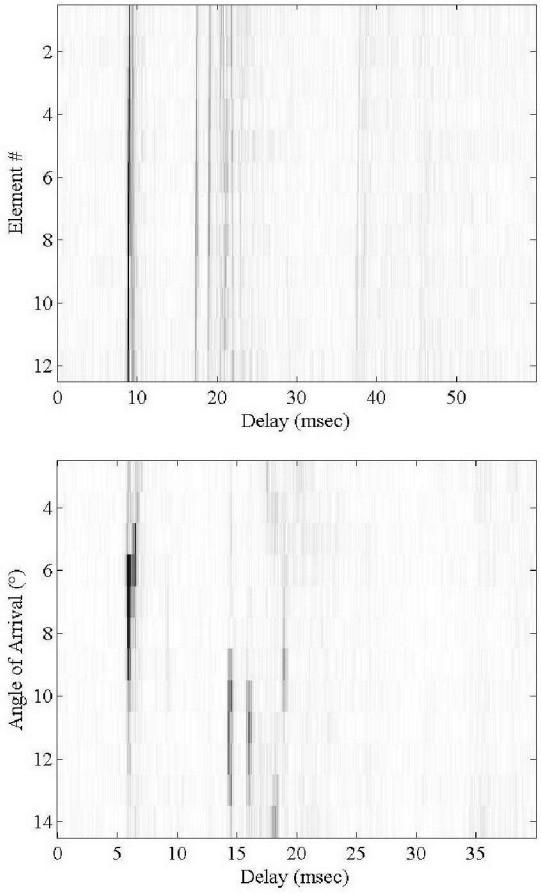

Figure 5. Channel impulse response amplitudes, as measured on rigid array for a high band signal at the North site, are shown. In the top panel, responses are for each array element while the bottom panel shows the response in beam space.

induced correlation between the signal stream estimates, each stream may be viewed as a parallel channel in the information theoretic sense. The capacity estimate, C, is then given as:

$$C = \sum_{\substack{parallel \\ channels}} \log_2\left(1 + SNR_{out}\right) \qquad (1)$$

Tables 1 and 2 provide these metrics for a group of mid-frequency band transmissions at the North and South site respectively. While the North site showed approximately a two-fold increase in capacity through the use of four transducers, the South site yield superior spatial modulation performance with over a three-fold increase in capacity. The two sites were explicitly chosen to provide a contrast in telemetry performance. This result, however, was counter to expectations prior to the test. With a hard bottom, the spatial structure of the acoustic field at the North site was thought to provide more potentially resolvable propagation paths while the soft bottom of the South site would deplete energy in ray paths other than the direct arrival. These results show the opposite to be true. This result suggests unexpected aspects of the acoustic propagation are deeply affecting spatial modulation performance.

A classical analysis for predicting performance in a MIMO channel would examine the value and distribution of the channel transfer function matrix singular values. For the tests considered in tables 1 and table 2, the average SNR per receiver element was nearly equivalent at 24 dB and 22 dB respectively. For the North site, the first four squared singular values are 20.5 dB, 17.5 dB, 14.7 dB, and 12.0 dB. For the South site, the first four values are 18.8 dB, 14.0 dB, 11.2 dB, and 6.0 dB. The classical conclusion would be that the North site is a better candidate for spatial modulation as it has a higher overall SNR and a more favorable singular value distribution. In fact, the opposite was found to be true. Two possible explanations will be considered.

Coherent UAC telemetry performance is often limited by residual inter-symbol interference (ISI). ISI typically results from an inability of the equalizer to estimate and compensate for channel dispersion. This may occur when the channel coherence time is less than the averaging time required to support reliable estimation. Spatial modulation is particularly sensitive to spatial coherence between the array elements. Figure 4 shows the array covariance matrix averaged over a 20 msec period for the low band transmission at both the North and South sites. As can be seen, the North site had markedly less coherence between the elements. The low-band array spacing (8 wavelengths) was chosen to increase the resolving power. In the light of these results, it is clear that care must be taken to balance the requirement for resolution with the need for coherence in designing appropriate arrays for spatial modulation. In the presence of frequency dispersion, optimization of array topology must account for coherence. For spatial modulation, the need for both receiver arrays and adequate time taps to cover late, spatially distinct arrivals puts pressure on the number of degrees of freedom. Stressing channel coherence times puts pressure on the required adaptation rate. These requirements are in conflict. One possible solution is a more compact data representation than delay and element taps.

A second explanation arises from a careful examination of the differing channel impulse responses. The hard bottom at the North site gave rise to an extended impulse response at 1.7 km range (figure 5, top panel). Significant energy continued to arrive 15 msec after the main arrival while weaker reverberant energy stretched out well beyond that. In contrast, the South site impulse response showed significant delay spreads of only 2 –3 msec. The delay spread is important

because successful spatial modulation requires that the equalizer be able to resolve the independent arrivals using the feedforward (as opposed to feedback) taps. In a time-varying channel, a performance penalty is generally incurred as the number of adapted degrees of freedom increase. Furthermore, with a sparse delay spread, an additional noise penalty is incurred for placing taps at delays with low signal energy. Once again, dispersion effects lead to degraded equalizer performance.

By considering the physical nature of the channel, however, one might expect the later arrivals to have unique angles of arrival. This observation suggests transforming the data from element space to angle-of-arrival space. Figure 5 (bottom panel) shows the beamformed impulse response at the North site. When the beamformer outputs are used rather than the element data streams directly, the equalizer is no longer encumbered with a lengthy delay spread in any given channel. For signals that are not spatially modulated, common practice would simply place feedback taps over the delayed arrivals. Spatial modulation, however, requires these late arrivals in the feedforward structure and benefits from this transformation. The benefit is clear when examining SNR_{out} for these two cases. Table 3 shows the performance of high band demodulation at 2.7 km range in the North location when the equalizer is run in element space. Table 4 shows the improvement when transformation to beam space is done prior to equalization. While the non-spatially modulated signal is only slightly affected, the improvement in the spatially modulated signals is pronounced especially for 3 channels, as the later arrival is made useful.

V. CONCLUSIONS

An effective receiver architecture has been presented that is suitable for decoding spatially modulated signals in the UAC. Using data collected jointly by the NATO Undersea Research Centre, SAIC, SPAWAR, the University of Delaware, and the Woods Hole Oceanographic Institution in the waters offshore of Elba, Italy, spatial modulation was shown to offer nearly a three-fold increase in capacity for the 9.6 – 12.4 kHz band and nearly a two-fold increase in capacity for the 25 – 35 kHz band. While the receiver architecture has features to compensate for channel dispersion, spatial modulation imposes unique requirements that make the algorithm more susceptible to performance degradation under severe dispersive conditions. Such conditions were shown be limiting performance in these tests rather than more classical criteria such as signal level or channel transfer function rank. Future work will consider algorithm modifications focused on these issues.

VI. ACKNOWLEDGEMENTS

The authors wish to acknowledge the support of the Office of Naval Research under the auspices of contracts N00014-97-1-0796 and N00014-01-C-0422. In addition, the data collection would not have been possible without the support of NATO Undersea Research Centre, the captain and crew of the R/V Alliance and the Saralu, and the dedicated technical staff of the Woods Hole Oceanographic Institution. We express our gratitude to Michael Porter, Martin Siderius, and Finn Jensen for the opportunity to participate in the test and all they did to make it a success.

Table 3. The demodulation performance for a hi-band signal sent in the North site at 2.0 km range is shown when the equalizer operates in element space.

	1 Chan	2 Chan	3 Chan
SNR_{out} (dB)	11.3	5.6	2.5
	-	4.4	1.3
	-	-	1.6
C	3.8	4.0	3.9

Table 4. The demodulation performance for a hi-band signal sent in the North site at 2.0 km range is shown when the equalizer operates in beam space.

	1 Chan	2 Chan	3 Chan
SNR_{out} (dB)	10.8	6.1	5.7
	-	6.1	5.8
	-	-	5.9
C	3.6	4.4	6.3

VII. REFERENCES

1. Kilfoyle, D. and A. Baggeroer, *The State of the art in underwater acoustic telemetry*. IEEE Journal of Oceanic Engineering, 2000. 25(1): p. 4-27.
2. Frisk, G.V., *Ocean and Seabed Acoustics: A Theory of Wave Propagation*. 1994, Englewood Cliffs: Prentice Hall. 299.
3. Stojanovic, M. et al., *Phase-coherent digital communications for underwater acoustic channels*. IEEE Journal of Oceanic Engineering, 1994. 19(1): p. 100-111.
4. Stojanovic, M. and Z. Zvonar, *Multichannel processing of broad-band multiuser communication signals in shallow water acoustic channels*. IEEE Journal of Oceanic Engineering, 1996. 21(2): p. 156-166.
5. Al-Dhahir, N., *Overview and comparison of equalization schemes for space-time-coded signals with application to EDGE*, IEEE Trans. on Signal Processing, 2002. 50(10): p. 2477-2488.
6. Duel-Hallen, A. and C. Heegard, *Delayed decision-feedback sequence estimation*. IEEE Trans. on Communicatiions, 1989. 37(5): p. 428-436.
7. Foschini, G. J., *Layered space-time architecture for wireless communication in a fading environment when using multiple antennas*. Bell Laboratory Technical Journal, 1996. 1(2): p. 41-59.

8. Ungerboeck, G., *Channel coding with multilevel/phase signals,* IEEE Trans. on Information Theory, 1982. 28(1).
9. Siwamogsatham, S. and M.P. Fitz, *Robust space-time codes for correlated Rayleigh fading channels.* IEEE Trans. on Signal Processing, 2002. 50(10): p. 2417-2428.
10. Jensen, F. B., et al., *Results from the Elba HF-2003 Experiment,* in High-Frequency Ocean Acoustics, Eds. M. Porter, M. Siderius, W. Kuperman, American Inst. Physics Press (2004).

Spatial Modulation in the Underwater Acoustic Channel

Daniel Kilfoyle, SAIC
Lee Freitag, WHOI
March 17, 2004

The Point of this Talk

- The waveguide-nature of the underwater acoustic channel (UAC) makes it well suited for spatial modulation. However, underwater acoustic telemetry often faces severe temporal and frequency dispersion as compared to what many RF wireless applications encounter.

- As RF MIMO efforts evolve (such as the DARPA Mobile Networked MIMO program), increasing bandwidth and mobility will emphasize the same issues currently faced by underwater acoustic MIMO channels. Thus, studying the UAC holds broader value for the communications community.

- Using data obtained during a 2003 at-sea test, three points will be made.

  - An effective receiver algorithm has been developed that can both handle "spatial demodulation" and substantive dispersion.

  - Time-varying channels with temporal dispersion may benefit from a pre-filter.

  - Coherence and resolvability can lead to opposing array design pressures.

Discussion Roadmap

- A review of the modulation approach and a MIMO DFE/PLL receiver structure
- A description of the at-sea testing conducted offshore of Elba, Italy
- A summary of spatial modulation results via post-equalization SNR and capacity.
- The impact of spatial coherence on spatial modulation performance
- The consequences and mitigation of excessive temporal dispersion

A Space-Time Coding Approach

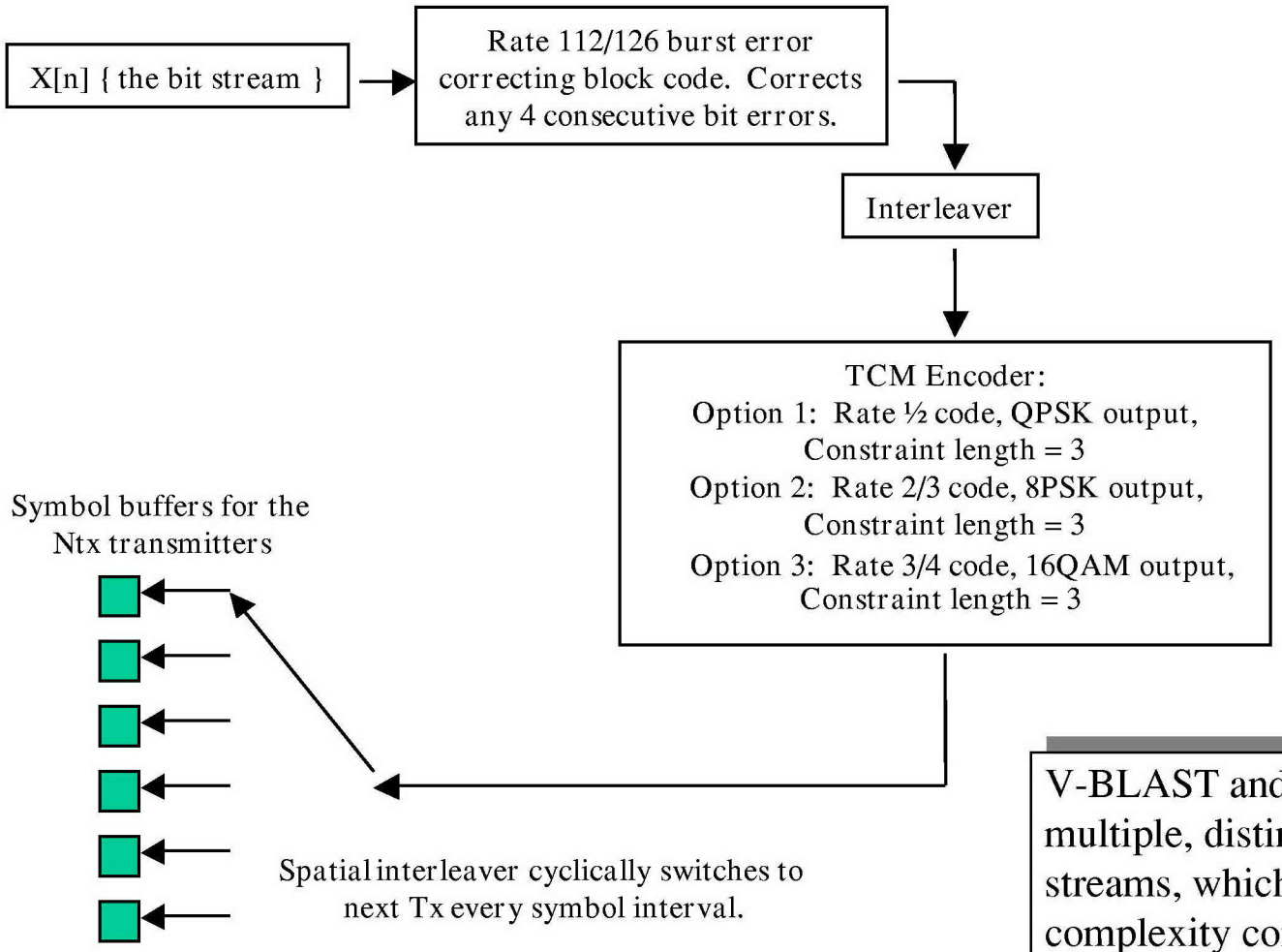

V-BLAST and D-BLAST use multiple, distinct coded bit streams, which is motivated by complexity concerns.

The Receiver Algorithm

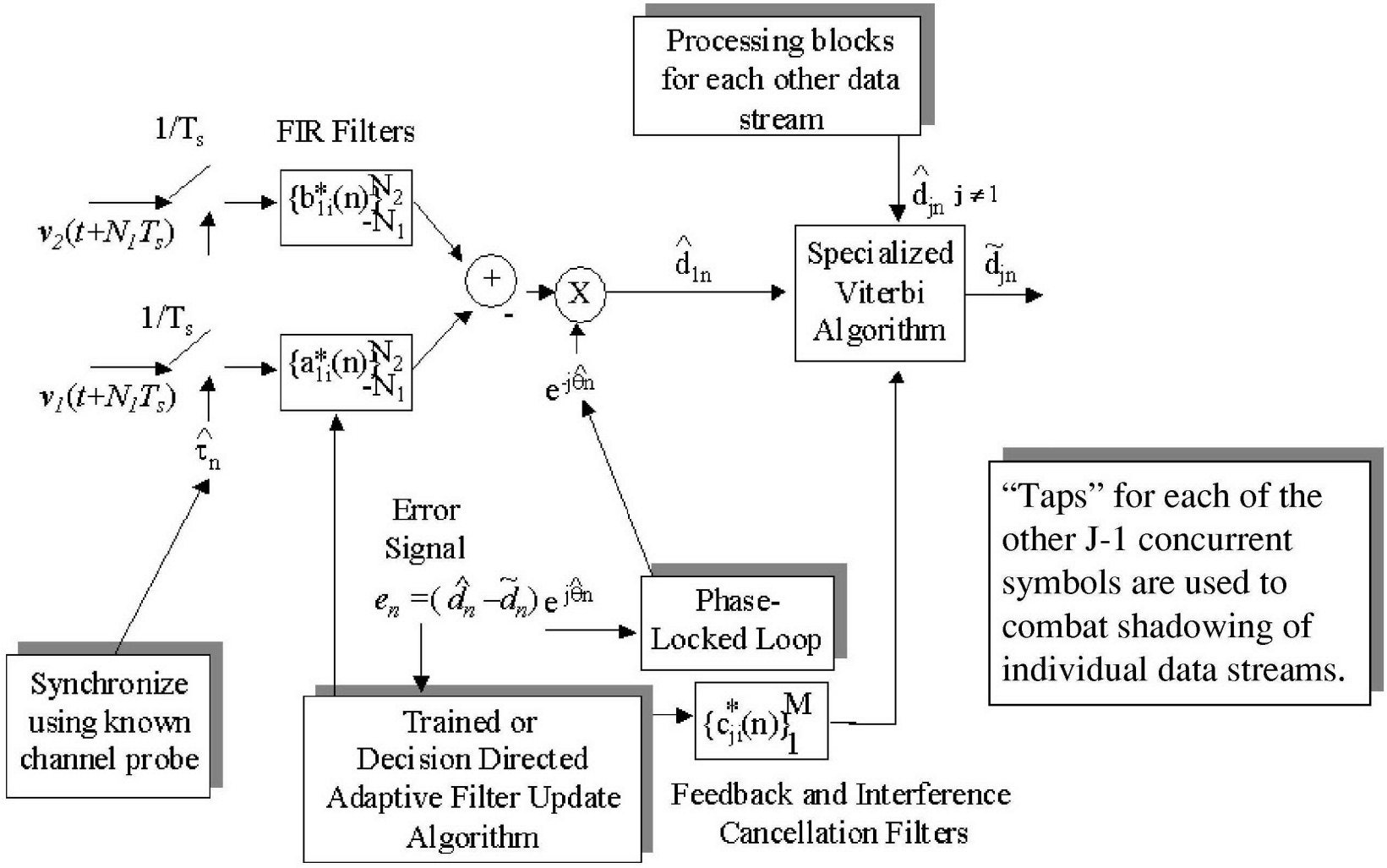

Elba-2003 Test Methodology

The Saralu'

Range varied from
0.8 km to 11 km

The Alliance

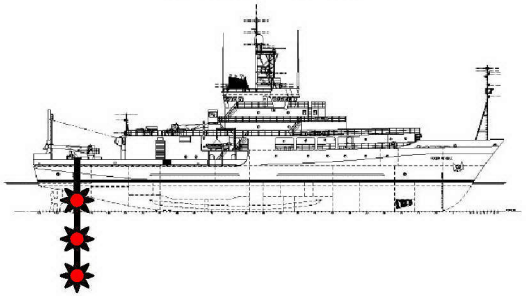

Source Equipment

6 Benthos AT-12ET transducers
- 9.5 to 14 kHz operating regime
- 2 meter spacing in VLA
- Coherent and independently driven

3 ITC-1032 transducers
- 25 to 35 kHz (only 6 dB loss up to 45 kHz)
- 21 inch spacing in VLA
- Coherent and independently driven

Receive Equipment

14 element flexible hydrophone VLA (1 m spacing)

12 element rigid hydrophone VLA (6 in spacing)

48 channel record capability at 48 kHz sampling rate

24 channel record capability at 96 kHz sampling rate

Data streamed to SCSI disk in WAV format enabling near real-time analysis

Elba-2003 Test Site

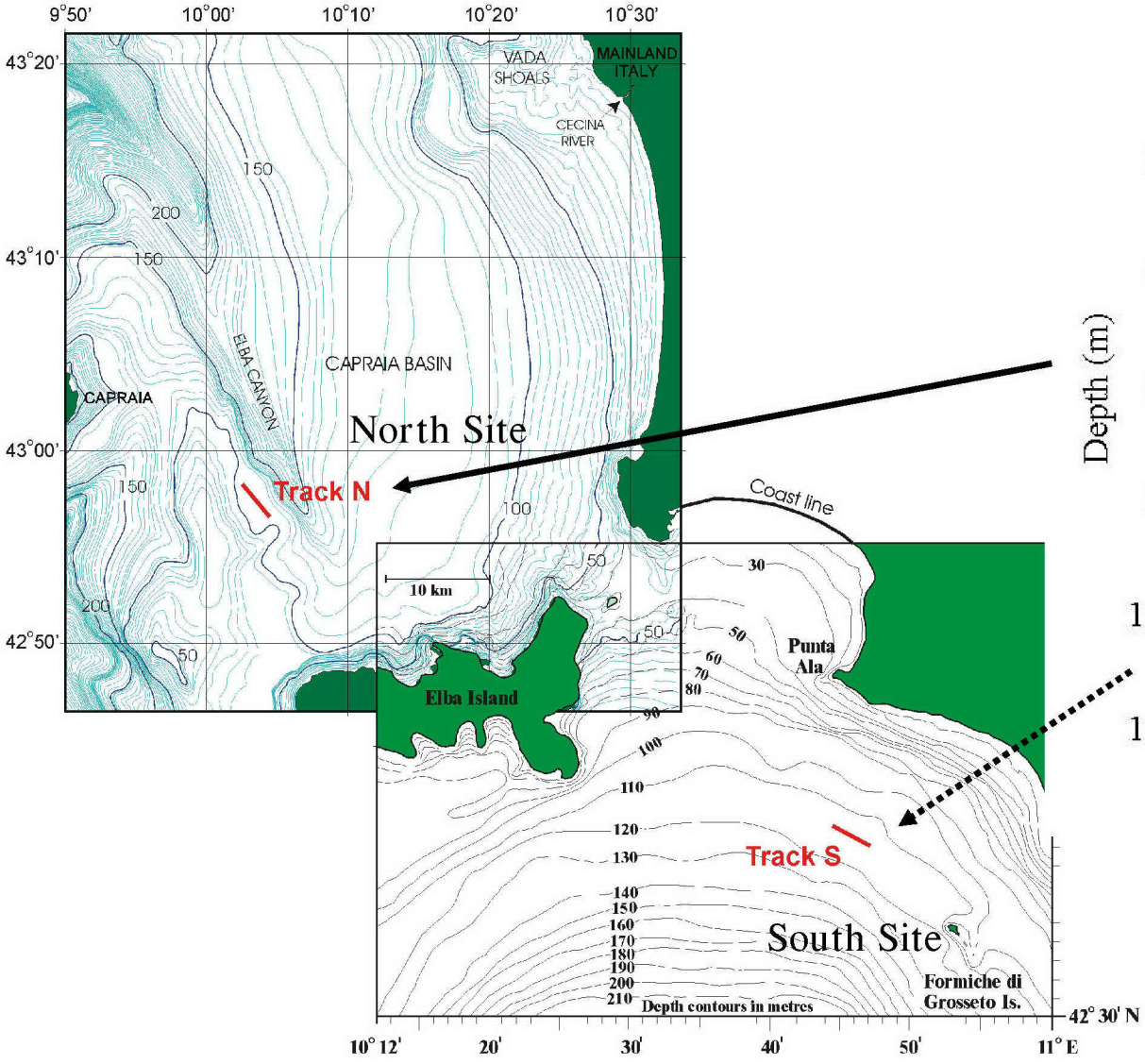

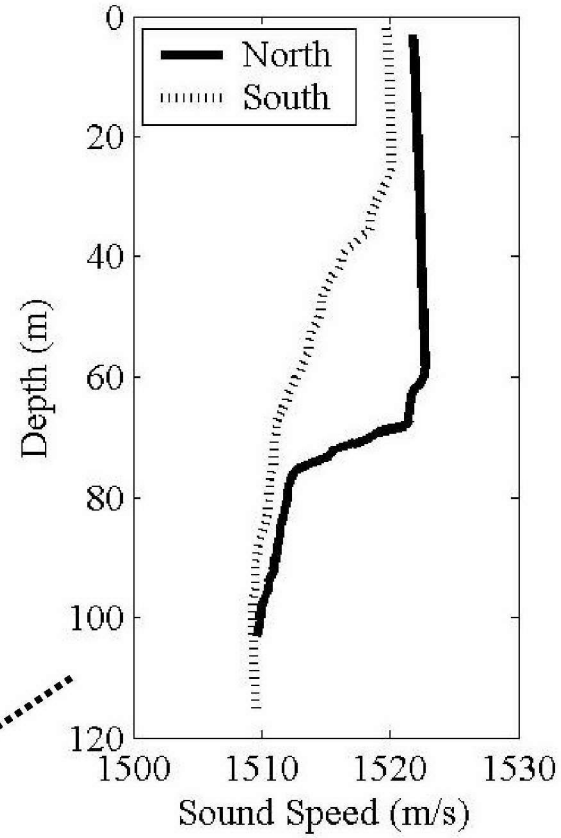

- *Graphic from HF Elba-03 post cruise test report.*

North Site Channel Responses: MF

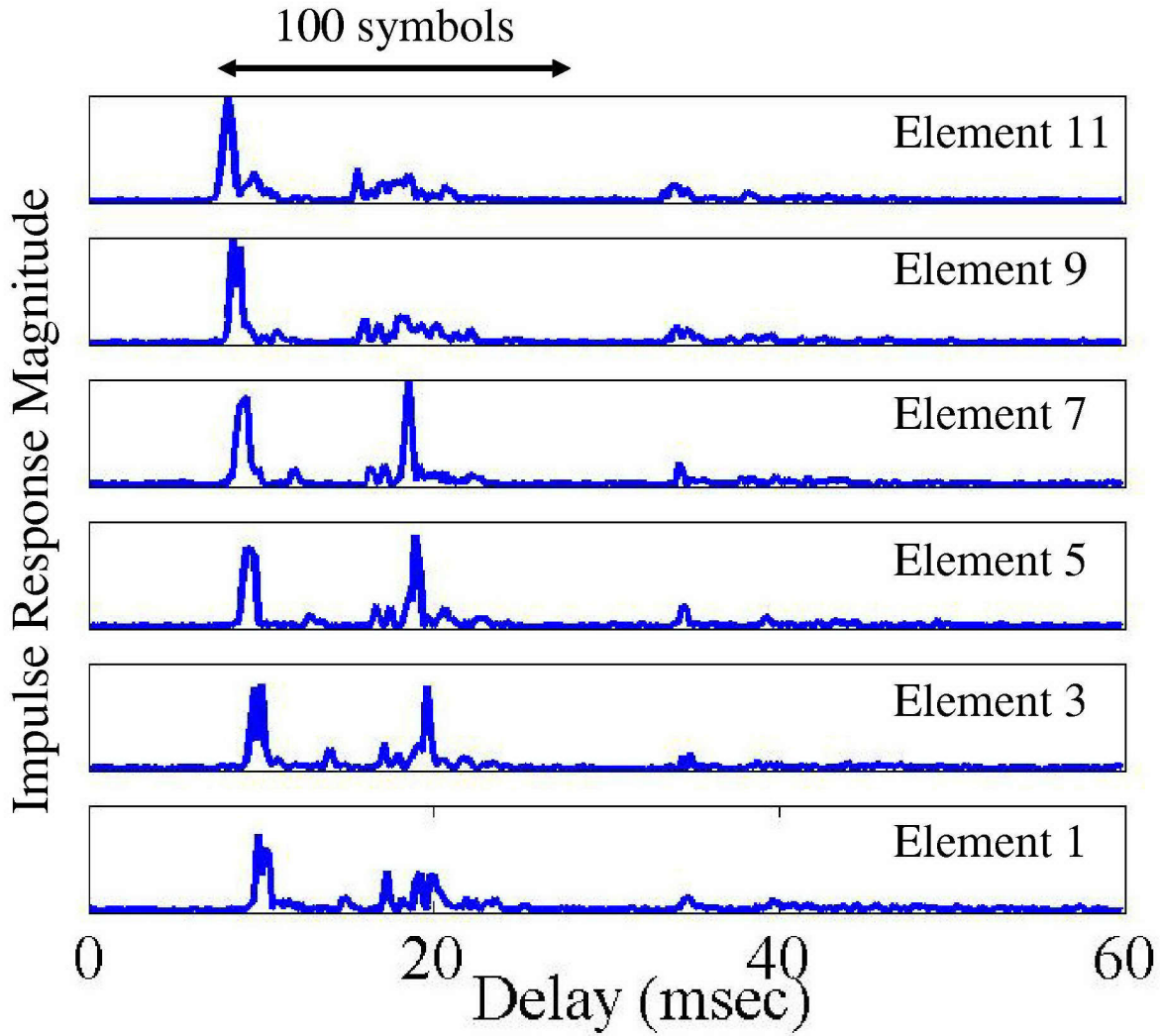

Freq.	9.5 – 14.5 kHz
Range	*2.1 km*
Tx	~20 m depth
Rx	~27 m depth

2 m spacing between every other element

** Estimates obtained with classical block least square estimation using about 0.5 seconds of data.*

South Site Channel Responses: MF

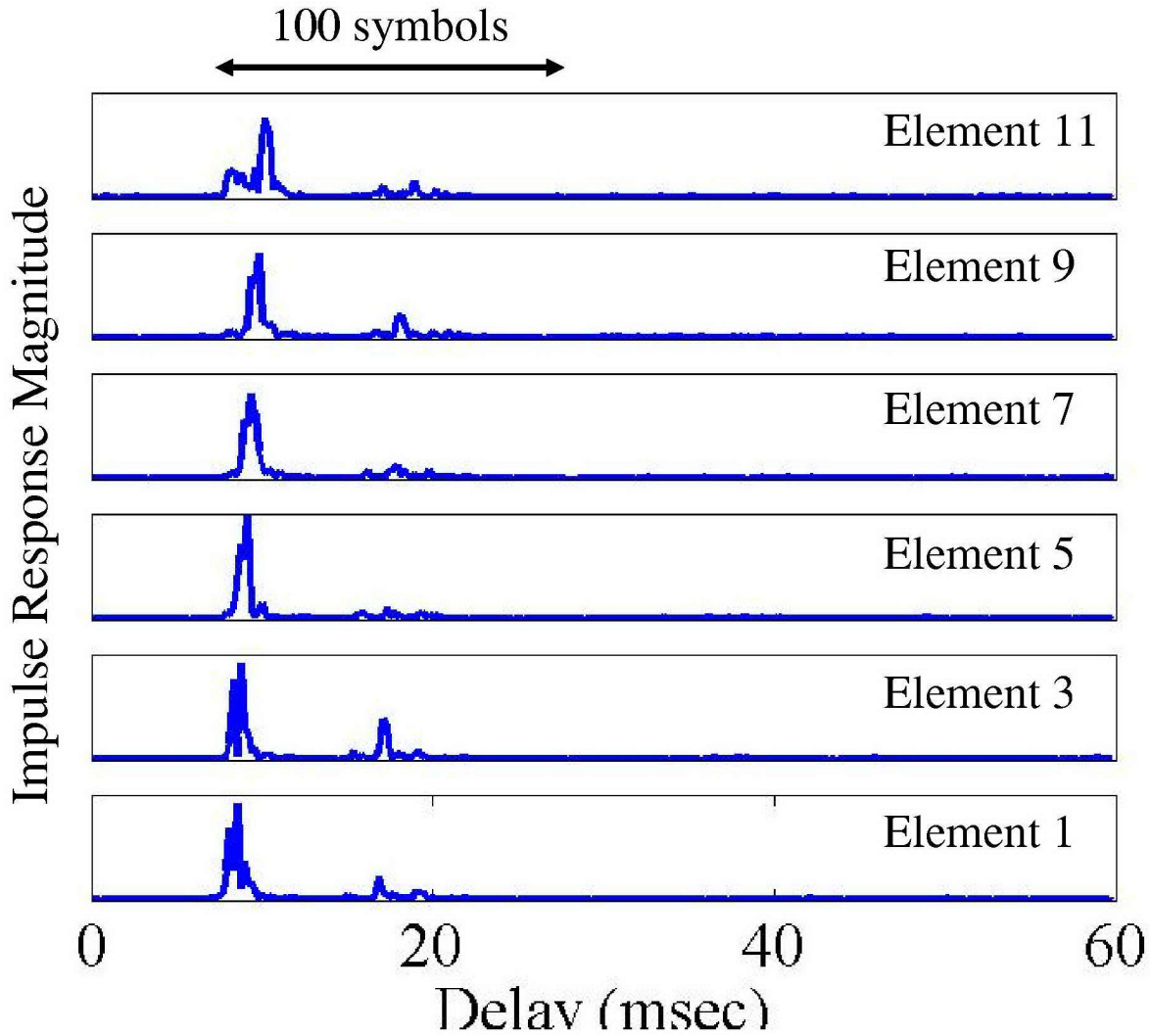

Freq.	9.5 – 14.5 kHz
Range	*2.5 km*
Tx	~20 m depth
Rx	~27 m depth

Spatial Modulation Performance

	1 Chan	2 Chan	3 Chan	4 Chan	5 Chan	6 Chan
SNR_{out} (dB)	16.1	11.4	8.7	7.4	5.3	3.7
	-	9.8	5.0	3.3	1.8	0.4
	-	-	7.7	5.9	2.3	1.6
	-	-	-	5.8	3.6	1.8
	-	-	-	-	4.3	3.0
	-	-	-	-	-	1.3
C	4.8	6.5	7.3	10.6	9.7	9.4

9.5 kHz – 14.5 kHz
2.1 km range at North Site
Collected on 14 element array
SNR_{in}/element ~ 27 dB

Similar signal levels and similar geometry but very different performance. Why?

Assume an additive, white Gaussian noise model for each parallel channel.

$$Capacity \equiv C = \sum_{\substack{parallel \\ channels}} \log_2\left(1 + SNR_{out}\right)$$

9.5 kHz – 14.5 kHz
2.7 km range at South Site
Collected on 14 element array
SNR_{in}/element ~ 30 dB

	1 Chan	2 Chan	3 Chan	4 Chan	5 Chan	6 Chan
SNR_{out} (dB)	23.5	19.1	16.3	13.0	9.1	6.0
	-	20.6	18.0	14.7	12.3	9.9
	-	-	17.2	13.8	11.3	5.0
	-	-	-	13.8	12.3	9.4
	-	-	-	-	8.4	3.9
	-	-	-	-	-	8.3
C	7.6	13.1	17.1	23.0	21.9	17.6

One Possible Answer: Spatial Coherence

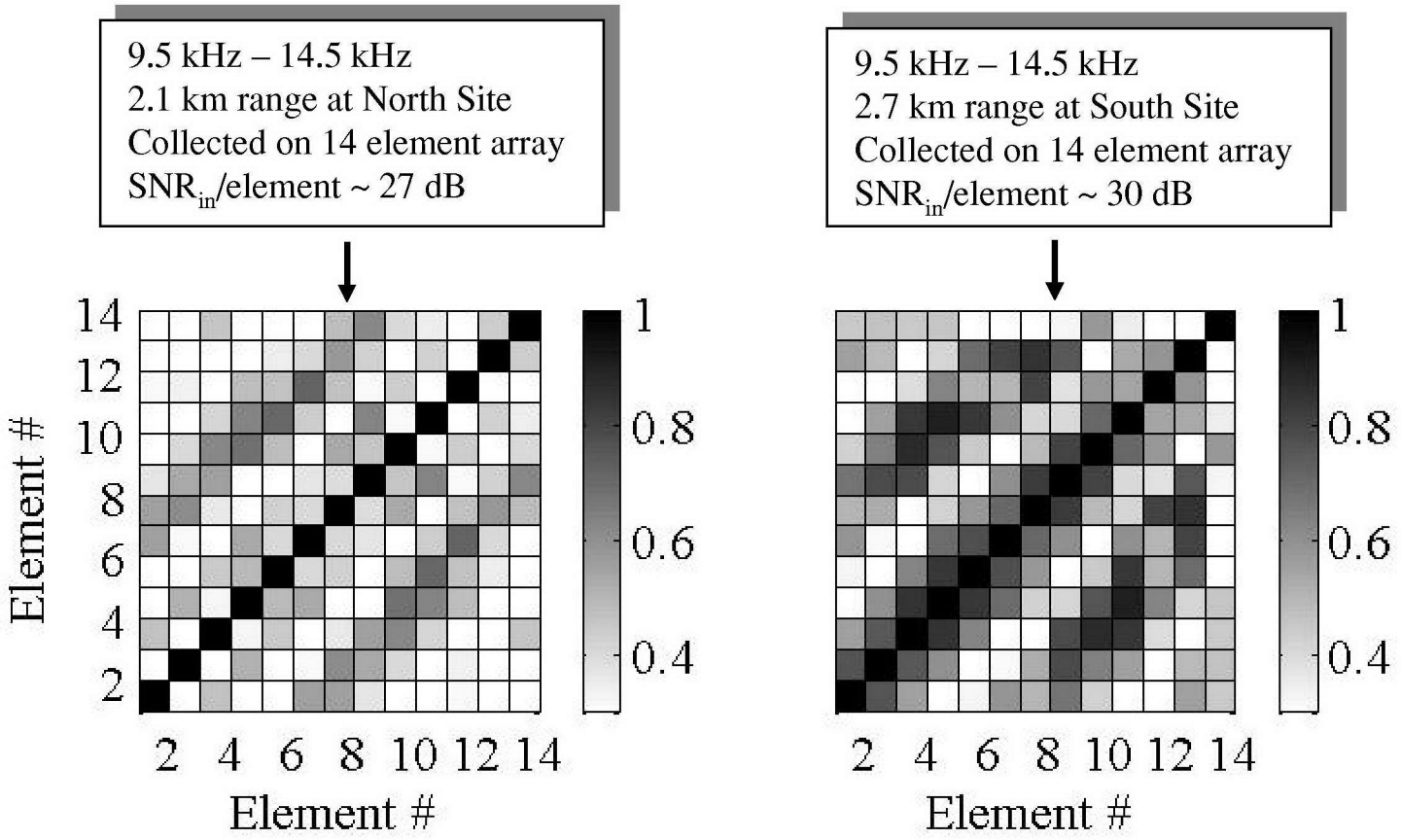

- *While the cause of the reduced coherence at the North site is a subject for another investigation, spatial modulation clearly requires spatial coherence over time scales of the adaptive filter update process.*
- *The competing issues of path resolvability and spatial coherence warrant further study.*

* Correlation matrix averaged over 300 symbols (60 msec).

Another Possible Answer: DoF Representation

Impulse Responses

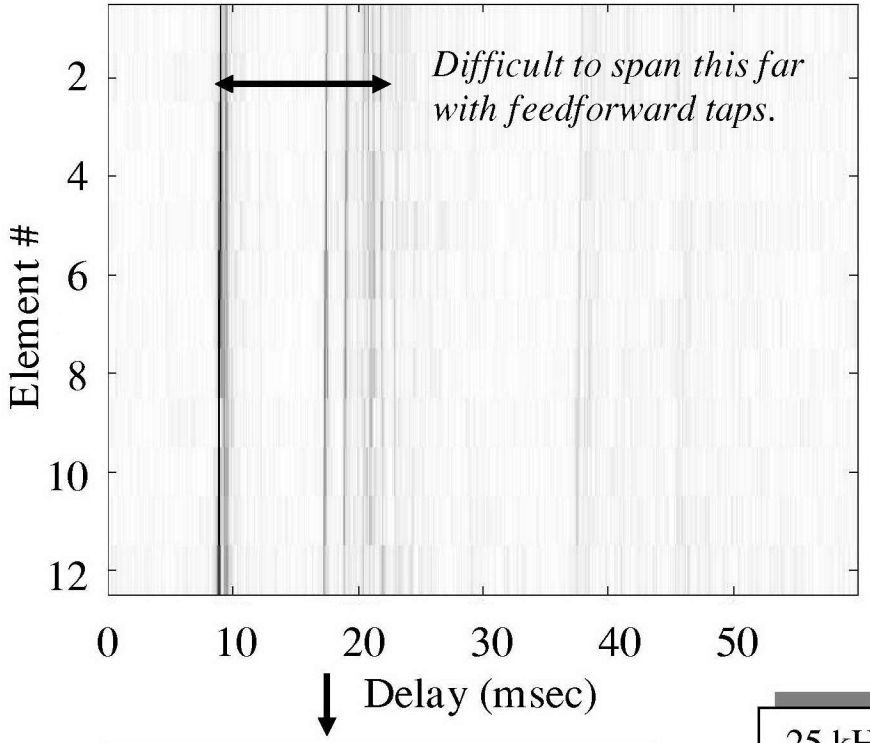

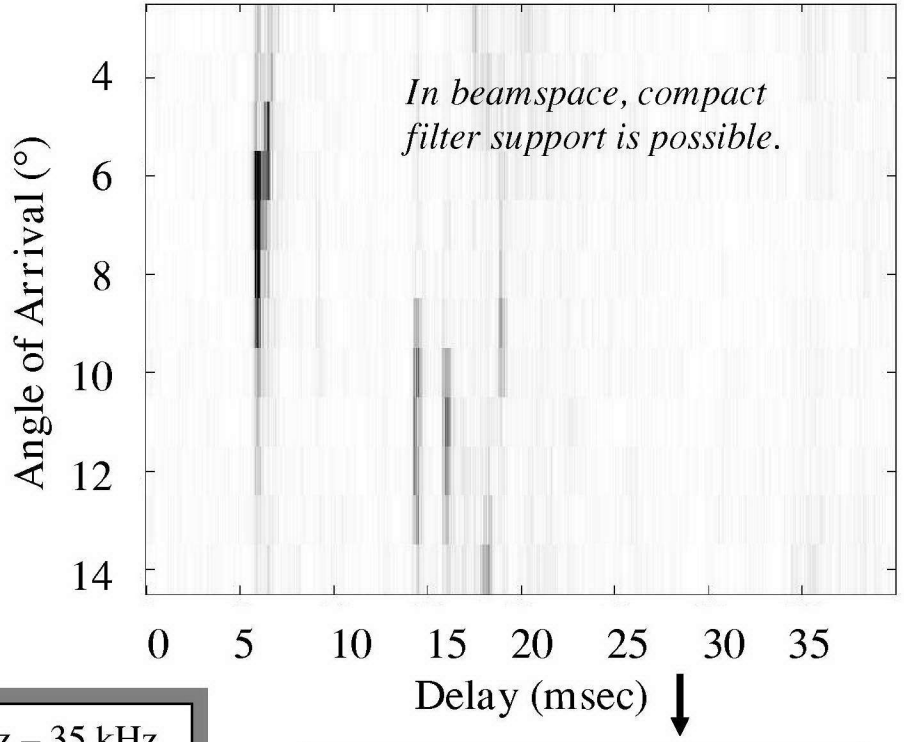

	1 Chan	2 Chan	3 Chan
SNR_{out} (dB)	11.3	5.6	2.5
	-	4.4	1.3
	-	-	1.6
C	3.8	4.0	3.9

25 kHz – 35 kHz
1.7 km range
North Site

	1 Chan	2 Chan	3 Chan
SNR_{out} (dB)	10.8	6.1	5.7
	-	6.1	5.8
	-	-	5.9
C	3.6	4.4	6.3

Closing Thoughts

- In this data set (and others), spatial modulation has been shown to offer two to three fold improvements in capacity, even when the channel is intersymbol interference limited and additional signal power is ineffective.
- Spatial coherence and multipath resolvability appear to impose opposing design constraints in the underwater acoustic channel. Bigger may not be better in dispersive MIMO channels.
- More compact representations of the signal space are particular important when the multipath (crucial for spatial modulation performance) is highly dispersed. Various sub-space based receiver algorithms may be indicated.
- The UAC may offer valuable insights for future terrestrial MIMO applications.
- We would like to acknowledge the support of ONR, the HF-Elba03 test team, and the NATO Undersea Research Centre.